KAPRI: A BISTATIC FULL-POLARIMETRIC INTERFEROMETRIC REAL-APERTURE RADAR SYSTEM FOR MONITORING OF NATURAL ENVIRONMENTS

Marcel Stefko[1], Othmar Frey[1,2], Charles Werner[2], Irena Hajnsek[1,3]

[1]Chair of Earth Observation and Remote Sensing, ETH Zurich, Switzerland
[2]GAMMA Remote Sensing, Gümligen, Switzerland
[3]Microwaves and Radar Institute, German Aerospace Center - DLR, Oberpfaffenhofen, Germany

IGARSS 2021 - 2021 IEEE International Geoscience and Remote Sensing Symposium | 978-1-6654-0369-6/21/$31.00 ©2021 IEEE | DOI: 10.1109/IGARSS47720.2021.9553427

ABSTRACT

In this submission the bistatic operation mode of KAPRI, a polarimetric-interferometric, ground-based, real-aperture, Ku-band, FMCW radar is presented. Its possible configurations and the synchronization procedures needed to achieve distortion-free single-look complex bistatic images are described. The challenges of polarimetric calibration in the bistatic regime are outlined, and a novel active calibration device and the associated polarimetric calibration method which are used for bistatic calibration of KAPRI are presented. First results of observations of natural environments (vegetation, snow) using bistatic KAPRI are shown.

Index Terms— Real-aperture radar, bistatic radar, polarimetry, polarimetric calibration, active radar calibrator, terrestrial radar, Ku-band radar

1. INTRODUCTION

Bistatic radar systems (i.e. systems in a configuration where the transmitter (Tx) and receiver (Rx) are spatially separated) are of research interest owing to their complementary properties to monostatic systems, such as possibility of recovery of 3-D displacement vectors, acquisition of long-baseline single-pass interferometric datasets [1], and measurements of bistatic radar cross-sections, which opens new possible pathways to recovery of biophysical parameters of the observed natural scenes [2].

Proliferation of bistatic radar systems is hindered by their increased complexity which leads to higher development and operational costs, since deployment of two independent – but synchronized – platforms is required for bistatic acquisitions. This is especially true for airborne and spaceborne sensors. Terrestrial devices, owing to their flexibility and lower costs, are an alternative well-suited for exploratory bistatic acquisitions and development of new observation methods, upon the results of which airborne and spaceborne missions can be designed and implemented. Furthermore, for small-scale applications, terrestrial sensors can offer denser temporal sampling (as opposed to spaceborne sensors) and longer observation periods (as opposed to airborne sensors), while keeping costs low.

Fig. 1: Bistatic KAPRI device configuration (left: primary device (P) equipped with narrow-beam traveling wave antennas, right: secondary receiver device (S) equipped with horn antennas). Reference link horn antennas are placed on tripods on the right side of the two images, together with long-range Wi-Fi antennas for remote device control.

Ground-based bistatic sensors (including SAR systems such as [3, 4]), while more limited in available observation geometries by local topography of the observed scene, offer a cost-efficient approach towards exploration of the bistatic parameter space, as well as possibilities for long-term monitoring of areas of interest with a high temporal sampling rate.

2. KAPRI

The monostatic operation mode and polarimetric calibration of KAPRI (Ku-band Advanced Polarimetric Radar Interferometer) has been introduced in [5]. KAPRI itself is an extension of the GAMMA Portable Radar Interferometer (GPRI) [6, 7] with fully-polarimetric capabilities. By synchronizing two KAPRI devices which were modified by GAMMA Remote Sensing to allow chirp synchronization, and increasing the beamwidth of the receiver device's antennas, we are able to perform bistatic acquisitions while preserving the high flexibility of the acquisition geometry. To the best of our knowledge, KAPRI is the first real-aperture, full-polarimetric, in-

terferometric, and bistatic radar system capable of monitoring areas kilometers in size with meter-scale resolution.

3. POSSIBLE CONFIGURATIONS

KAPRI offers two possible configurations for bistatic acquisitions, based on the desired length of the bistatic baseline:

1. For (relatively) narrow bistatic baselines, KAPRI's 100 MHz reference clock signal can be directly transmitted between the two devices using a coaxial cable. This then means that both devices are effectively driven by the same reference clock, which eliminates drift effects which would be caused by deployment of two free-running clocks. However, since losses in coaxial cables increase exponentially with length, this method can only be deployed at relatively narrow bistatic baselines up to 100 m.

2. To achieve a wider range of bistatic baselines (and resulting bistatic angles), long bistatic baselines (up to several kilometers in length) can be achieved via deployment of a Ku-band link, where approximately 10 % of chirp power is transmitted directly from the transmitter to the receiver. This directly transmitted signal is used to correct phase and frequency offsets caused by the fact that the two devices are driven by two independent reference clocks.

The two configurations are visualized in Fig. 2, with their differences highlighted in red and blue respectively.

4. BISTATIC POLARIMETRIC CALIBRATION

The monostatic version of KAPRI uses a trihedral corner reflector combined with the reciprocity principle to compute the four necessary calibration parameters f, g, ϕ_r, ϕ_t [5]. However, neither trihedral corner reflectors, nor the reciprocity principle can be applied in bistatic measurements. A new method thus had to be developed to compute these parameters in the bistatic configuration.

Similarly to other bistatic devices [8, 9], we employ an active calibration target, combined with a suitable calibration method.

4.1. Active calibration target

Our design of the calibrator VSPARC (Variable Signature Polarimetric Active Radar Calibrator) employs two horn antennas with a Ku-band amplifier in-between. This ensures sufficient RCS for calibration even in presence of background clutter, and a low weight. Directional flexibility and ease of alignment is provided by custom-made mounting adapters for the antennas – a manually-operated camera mount is used for pointing the antennas in the direction towards the transmitting and receiving radars. Afterwards, polarization of the antennas

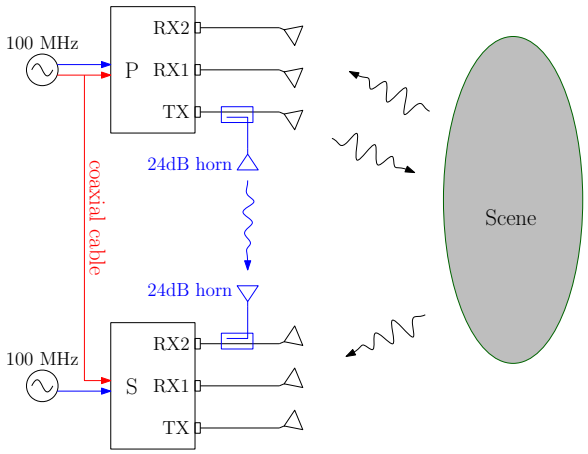

Fig. 2: Diagram of bistatic KAPRI device configuration, and the two possible synchronization options. Elements only present in narrow-baseline configuration (employing cable synchronization) are highlighted in red, while elements only present in wide-baseline configuration (employing a Ku-band synchronization link) are highlighted in blue. To observe the scene, the primary device (P) employs high-gain (32 dB) slotted-waveguide antennas, while the secondary device (S) employs 20 dB horn antennas.

can be adjusted by physical rotation around their line of sight, provided by a rotation stage. The mounting adapter is designed in a way such that the phase center of the antenna lies on the central axis of the rotation stage - changing the polarization of the antenna can be thus done without introducing any additional significant phase offsets.

The scattering matrix of the calibrator can then be derived as

$$\mathbf{S}_{\text{cal}} = e^{j\phi_{\text{abs}}(\varphi_{\text{T}},\varphi_{\text{R}})}\sqrt{G}\begin{bmatrix}\sin\varphi_{\text{T}}\sin\varphi_{\text{R}} & \cos\varphi_{\text{T}}\sin\varphi_{\text{R}}\\ \sin\varphi_{\text{T}}\cos\varphi_{\text{R}} & \cos\varphi_{\text{T}}\cos\varphi_{\text{R}}\end{bmatrix} \quad (1)$$

where G, is the gain of the calibrator, $\varphi_{\text{T}}, \varphi_{\text{R}}$ are the rotational positions of the antennas aimed at the transmitter and receiver respectively, and $\phi_{\text{abs}}(\varphi_{\text{T}}, \varphi_{\text{R}})$ is the absolute phase delay term, which depends on cable length and precise position of the antennas. The exact values of individual elements of the scattering matrix can thus be altered by changing the rotational position of the antennas.

4.2. Polarimetric calibration method

By performing measurements of the scattering matrix of the VSPARC device in multiple configurations of its antennas, we can now compute the four polarimetric calibration parameters. We denote as $K_{\text{XY}}^{\varphi_{\text{R}},\varphi_{\text{T}}}$ the measurement of the XY-element of the calibration device's scattering matrix while the antennas of the device are in positions $\varphi_{\text{R}}, \varphi_{\text{T}}$. Then, the four

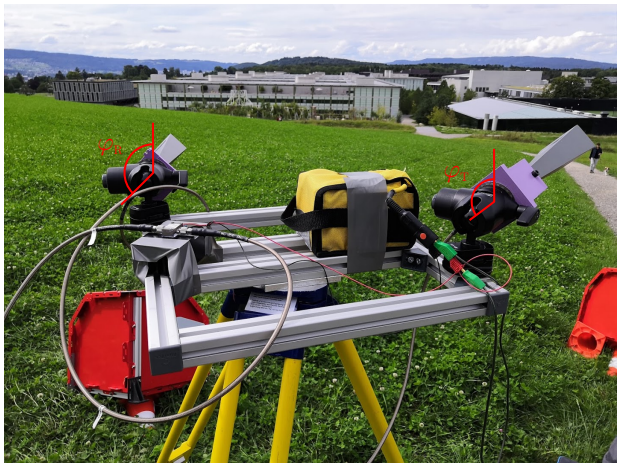

Fig. 3: VSPARC device deployed in the field. Antennas are pointed at KAPRI devices and customized 3D-printed adapters enable rotation of antennas around their pointing axis without significantly affecting the position of the phase center.

calibration parameters can be computed as:

$$f = \sqrt{\left| \frac{K_{\mathrm{VV}}^{0°,0°}}{K_{\mathrm{HH}}^{90°,90°}} \right|} \tag{2a}$$

$$g = \sqrt{\left| \frac{K_{\mathrm{HV}}^{90°,0°}}{K_{\mathrm{VH}}^{0°,90°}} \right|} \tag{2b}$$

$$\phi_r = \arg\left(\frac{K_{\mathrm{VH}}^{45°,45°}}{K_{\mathrm{HH}}^{45°,45°}} \right) \tag{2c}$$

$$\phi_t = \arg\left(\frac{K_{\mathrm{HV}}^{45°,45°}}{K_{\mathrm{HH}}^{45°,45°}} \right) \tag{2d}$$

5. RESULTS

Table 1 shows the comparison between retrieved calibration coefficients using the old and new method.

Table 1: Comparison of retrieved calibration coefficients for old (monostatic) method on corner reflectors CR1 and CR2 and new (bistatic) method on calibration device VSPARC.

	f	g	$\phi_t[°]$	$\phi_r[°]$
CR1	0.95 ± 0.01	0.97 ± 0.01	-100.7 ± 0.6	12.9 ± 0.3
CR2	0.95 ± 0.01	0.98 ± 0.01	-90.3 ± 1.0	22.4 ± 0.7
VSPARC	0.92 ± 0.02	0.99 ± 0.01	-90.1 ± 0.8	11.9 ± 1.2

6. DISCUSSION

Table 1 demonstrates that the calibration coefficients returned by the novel active calibration method (VSPARC) match the values returned by the previously validated monostatic method (CR1, CR2). The active method thus allows us to extend the polarimetric calibration capabilities into the bistatic regime, independent of bistatic angle.

Full polarimetric-interferometric capabilities of bistatic KAPRI, combined with its flexibility in temporal sampling rates and coverage periods, open up possibilities for investigations in several areas:

- Displacement monitoring: The bistatic attachment of KAPRI can enhance the displacement-monitoring capabilities of GPRI by providing access to the value of displacement along a second line-of-sight vector. This allows for the recovery of 3-dimensional displacement vector maps.

- Top-layer vegetation monitoring: Past research has demonstrated sensitivity of Ku-band radar to biophysical properties of top-layer vegetation. Investigation of bistatic polarimetric signatures of vegetation over the growth cycle might improve on this method. Fig. 4 shows a comparison between calibrated monostatic and bistatic polarimetric images of a vegetation-covered area.

- Snow and ice: Certain scattering phenomena occurring in snow and ice layers are only detectable in the bistatic regime, such as the coherent backscatter opposition effect [10]. As a portable real-aperture fully polarimetric bistatic system, KAPRI can be used to probe this phenomenon in the Earth's cryosphere (see Fig. 5).

7. REFERENCES

[1] A. Moreira, G. Krieger, I. Hajnsek, K. Papathanassiou, M. Younis, P. Lopez-Dekker, S. Huber, M. Villano, M. Pardini, M. Eineder, F. De Zan, and A. Parizzi, "Tandem-L: A Highly Innovative Bistatic SAR Mission for Global Observation of Dynamic Processes on the Earth's Surface," *IEEE Geoscience and Remote Sensing Magazine*, vol. 3, no. 2, pp. 8–23, 2015.

[2] K. B. Khadhra, T. Boerner, D. Hounam, and M. Chandra, "Surface parameter estimation using bistatic polarimetric x-band measurements," *Progress In Electromagnetics Research B*, vol. 39, no. 39, pp. 197–223, 2012.

[3] S. Wang, W. Feng, K. Kikuta, G. Chernyak, and M. Sato, "Ground-based bistatic polarimetric interferometric synthetic aperture radar system," in *IGARSS 2019-2019 IEEE International Geoscience and Remote Sensing Symposium*. IEEE, 2019, pp. 8558–8561.

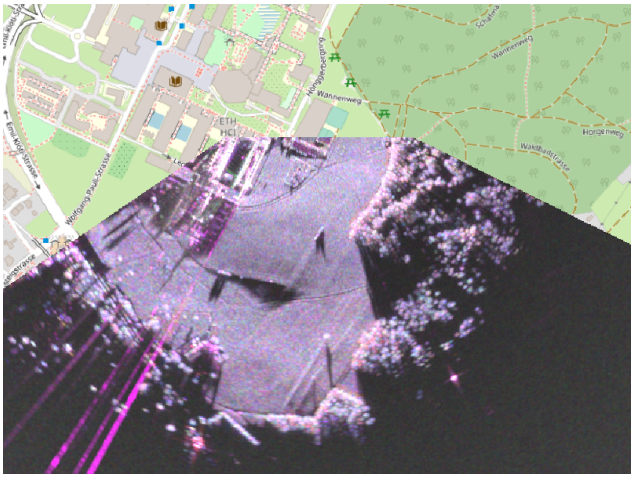

(a) Monostatic image. The primary device was placed on top of a building and thus had very good line of sight over the observed area.

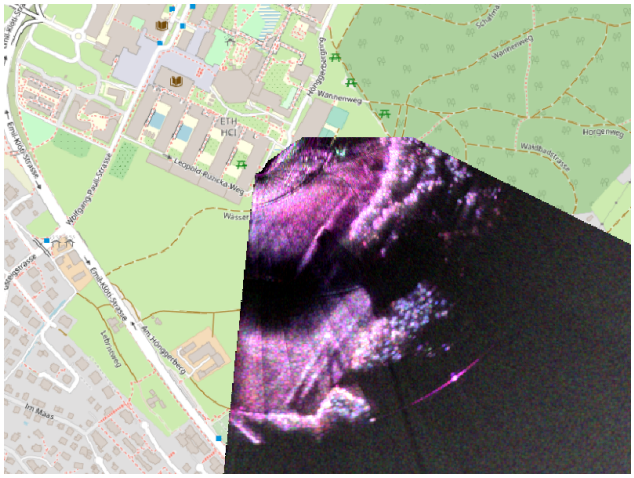

(b) Bistatic image. Mosaicking of multiple acquisitions was required in order to achieve coverage comparable to the monostatic acquisition. This causes radial "stripes" to appear in the image, which is a mosaicking artifact caused by the modulation of intensity by the receiver antenna pattern. This only affects radiometric information – relative intensities and phases between individual polarimetric channels are preserved.

Fig. 4: Comparison of the monostatic polarimetric image acquired by the primary device (left), and bistatic image acquired by the secondary device (right). Polarimetric data is presented in the Pauli color basis (R: HH-VV, G: HV, B: HH+VV). Map data source: OpenStreetMap.

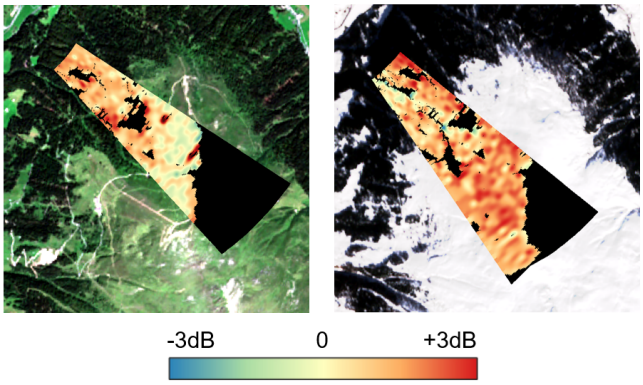

Fig. 5: Application of bistatic KAPRI to observe a narrow backscatter enhancement peak in dry snow on top of the peak Rinerhorn in Davos, Switzerland. The color represents the difference of measured bistatic backscatter intensity between acquisitions performed at baselines of $2\,\mathrm{m}$ and $50\text{-}55\,\mathrm{m}$. On the exposed part of the hill, no significant backscatter difference is present in summer (left). In winter, the same part of the hill covered in snow (right) exhibits a significant change in the backscatter, suggesting the presence of coherent backscatter opposition effect. Map underlay: Modified Copernicus Sentinel data 2020/Sentinel Hub

[4] M. Pieraccini and L. Miccinesi, "Bistatic GBSAR for detecting target elevation," in *2017 IEEE International Conference on Microwaves, Antennas, Communications and Electronic Systems (COMCAS)*. IEEE, 2017, pp. 1–4.

[5] S. Baffelli, O. Frey, C. Werner, and I. Hajnsek, "Polarimetric calibration of the Ku-band Advanced Polarimetric Radar Interferometer," *IEEE Transactions on Geoscience and Remote Sensing*, vol. 56, no. 4, pp. 2295–2311, 2017.

[6] C. Werner, A. Wiesmann, T. Strozzi, A. Kos, R. Caduff, and U. Wegmuller, "The GPRI multi-mode differential interferometric radar for ground-based observations," in *EUSAR 2012; 9th European Conference on Synthetic Aperture Radar*. VDE, 2012, pp. 304–307.

[7] T. Strozzi, C. Werner, A. Wiesmann, and U. Wegmuller, "Topography mapping with a portable real-aperture radar interferometer," *IEEE Geoscience and Remote Sensing Letters*, vol. 9, no. 2, pp. 277–281, 2011.

[8] D. R. Brunfeldt and F. T. Ulaby, "Active reflector for radar calibration," *IEEE Transactions on Geoscience and Remote Sensing*, , no. 2, pp. 165–169, 1984.

[9] M. Pienaar, J. W. Odendaal, J. Joubert, J. Cilliers, and J. Smit, "Active calibration target for bistatic radar cross-section measurements," *Radio Science*, vol. 51, no. 5, pp. 515–523, 2016.

[10] S. Tan, W. Chang, L. Tsang, J. Lemmetyinen, and M. Proksch, "Modeling Both Active and Passive Microwave Remote Sensing of Snow Using Dense Media Radiative Transfer (DMRT) Theory with Multiple Scattering and Backscattering Enhancement," *IEEE Journal of Selected Topics in Applied Earth Observations and Remote Sensing*, vol. 8, no. 9, pp. 4418–4430, 2015.